LOW HORIZONTAL BETA FUNCTION IN LONG STRAIGHTS OF THE NSLS-II LATTICE *

F.Lin#, J.Bengtsson, W.Guo, S.Krinsky, Y.Li, L.Yang, BNL, NY, 11973 USA

Abstract

The NSLS-II storage ring lattice is comprised of 30 DBA cells arranged in 15 superperiods. There are 15 long straight sections (9.3m) for injection, RF and insertion devices and 15 short straights (6.6m) for insertion devices. In the baseline lattice, the short straights have small horizontal and vertical beta functions but the long straights have large horizontal beta function optimized for injection. In this paper, we explore the possibility of maintaining three long straights with large horizontal beta function while providing the other 12 long straights with smaller horizontal beta function to optimize the brightness of insertion devices. Our study considers the possible linear lattice solutions as well as characterizing the nonlinear dynamics. Results are reported on optimization of dynamic aperture required for good injection efficiency and adequate Touschek lifetime.

INTRODUCTION

For the NSLS-II baseline storage ring lattice [1] with 30 DBA cells, long straights with large horizontal beta functions are located at the even number cells, and short straights with small horizontal and vertical beta function are located at the odd number cells. Specifically, injection point is located at the 30th cell; three damping wigglers (DW) are located at the 8th, 18th and 28th cell for 3-fold symmetry; RF straights are currently located at the 22nd (and 24th cell for more insertion devices). Large horizontal beta function in the long straight provides adequate horizontal space for beam injection. However, this increases the horizontal beam size, which impairs the brightness of the insertion devices. For further lattice development, we would like to preserve the baseline lattice properties, like large horizontal beta function in one long straight for injection, while reduce it in some other long straights for the optimization of brightness.

Considering the fixed position of injection and damping wigglers (DW) and keeping the ring with a high order symmetry, a reasonable 3-fold symmetric ring layout is presented in Figure 1, where LSH represents long straight with high horizontal beta function and LSL represents long straight with low horizontal beta function. In this type of allocation, the injection point at LSH can maintain large horizontal beta function for the beam injection. The significant advantage from this modified ring lattice is that low horizontal beta function in the LSL optimizes the brightness of damping wigglers and insertion devices.

LINEAR OPTICS OPTIMIZATION

The study starts from the baseline lattice functions as shown below in Figure 2. The lattice modification will follow guidelines that were applied for the original design

*Work supported by U.S. DOE contract No. DE-AC02-98CH10886
#flin@bnl.gov

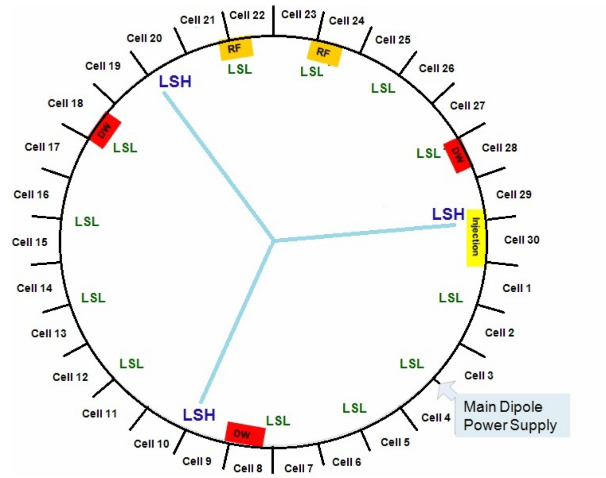

Figure 1: The modified storage ring layout with 3-fold symmetry. LSH represents long straight with high horizontal beta function; LSL represents long straight with low horizontal beta function.

[1, 2]: ~2nm-rad natural emittance without damping wigglers and 3-pole wigglers, horizontal chromaticity ~105 in magnitude (~6.9 per supercell i.e. 2 DBA cells), β_x ~3 m and β_y ~1 m at the center of the short straight sections. Symmetry conditions are maintained at the center of the straights and at the center of the arcs. The DBA is achromatic so that the linear dispersion is zero in all of the straight sections. The maximum dispersion is at the center of the arc and is ~0.46 m which facilitates chromaticity correction with reasonable sextupole strength.

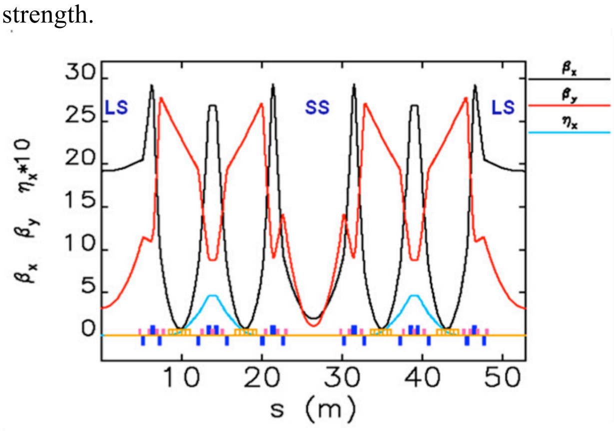

Figure 2: The baseline lattice functions for two DBA cells (LS: long straight; SS: short straight).

Since only the beta function in the long straight needs to change significantly, first study was carried out to explore what could be achieved by only changing the strengths of the three existing QH quadrupole families bounding the long straights. The strength (B'/B) of QHs is practically constrained to be less than 2.2 /m^{-2}. In tuning the lattice, we applied constraints to make the lattice symmetric at the center of the straight section $(\alpha_x = \alpha_y = 0)$ and scanned β_x from 1 m to 20 m at the center of the long straight. We note that at the center of the long straight the vertical beta functions change slightly when the horizontal beta functions vary from 1-20 m as shown in Figure 3. For the desired value of β_y ~3 m, the horizontal beta function can be either ~2 m or ~20 m. Therefore we see that we can pursue small β_x ~2 m for the IDs.

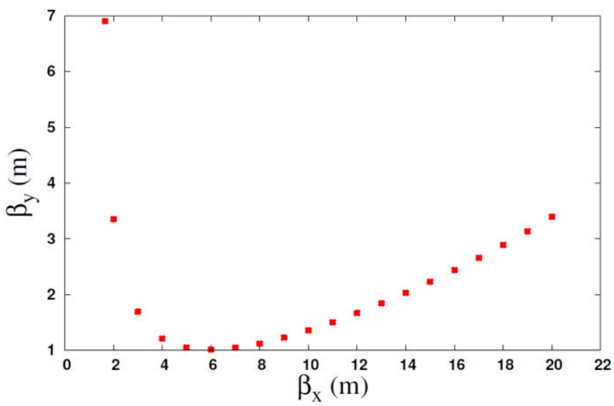

Figure 3: Dependence of the vertical beta function on the value of the horizontal beta function, both evaluated at the center of the long straight.

For all of the horizontal beta function scans, the emittance barely changes because the achromat remains untouched. At the desired values of beta functions, β_y~3 m and small β_x~2m, the natural horizontal chromaticities of this 2 DBA cells do not exceed a magnitude of 7 as given in Figure 4. This indicates that we may provide the desired linear optics while optimizing sextupoles with modest strength. To control the tunes to achieve specific working points, the other quadrupoles families QLs bounding the short straights and QMs in the arcs between the dipole magnets need to be adjusted globally.

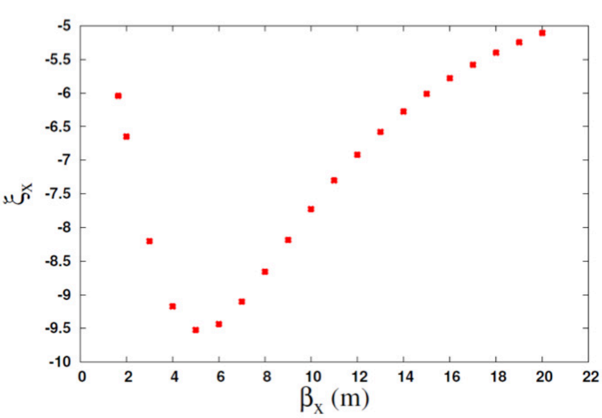

Figure 4: The horizontal chromaticity per 2 DBAs vs. Horizontal beta function at the center of the long straight.

NONLINEAR OPTIMIZATION

Both linear and nonlinear properties of the lattice determine the dynamic aperture, which must be large enough for good injection efficiency and sufficient Touschek lifetime. From the linear optimization point of view, moving the working point away from the leading order resonance lines is an important consideration. Meanwhile, to avoid the sextupoles becoming too strong, the linear lattice should be designed with horizontal chromaticity < 110 in magnitude for the whole ring and with peak dispersion ~0.46m [1].

For the nonlinear optimization 9 sextupoles families in each DBA cell are available. Among them 3 sextupoles families are located in the non-zero dispersion region. Two of them are determined to correct the first-order chromaticity and the remaining one, together with the other 6 sextupoles located in the zero-dispersion region, are used to compensate the second-order chromaticity, tune shift with amplitude and nonlinear resonance driving terms. For our present study of the lattice composed of high and low horizontal beta long straights and DWs, some of sextupole families are released to increase the freedom degree. Therefore, the whole storage ring has 21 different sextuples families available for the nonlinear optimization.

Elegant [3] provides the simulation platform for the nonlinear optimization used in this paper. Tuning the sextupole families, analytic expressions [4, 5] for the driving terms of resonances are calculated, and the penalty function is calculated as a weighted sum of linear and nonlinear chromaticity, resonance and tune shift with amplitude related terms. The dynamic aperture is optimized by using this approach.

For the most realistic situation, the dynamic aperture must be obtained by considering errors, such as magnet misalignment [6], and physical aperture. Instead of modelling large errors plus corrections, we can simply use random errors that result in lattice functions with errors at a corrected level. At NSLS-II, the horizontal aperture comes from the photon absorbers (±38 mm), and the vertical apertures are limited by the insertion devices (IDs) due to the vertical gaps. For instance, the minimum vertical gap of IDs is 5 mm of IVU U20 located at the center of short straight (SS). The calculations of frequency maps presented in the next section include realistic magnet misalignment errors and physical aperture along the whole storage ring.

OPTIMIZATION RESULTS

A lattice with working point (37.18, 16.2) is optimized to obtain good dynamic aperture. The lattice functions for 1/3 of the ring are plotted in Figure 5.

Frequency maps in the (x,δ) and (x,y) space are computed by considering both the magnet misalignments and physical apertures. Figure 6 shows the tune change for particles with y=1 mm, |x|<~20 mm and momentum deviation up to ±3% in the (x,δ) space. Figure 7 shows the tune change for on-momentum particles with different initial transverse postions in the (x,y) space [7]. The maps are plotted in terms of tune diffusion, which is defined as $\log_{10}^{(\Delta\upsilon_x^2+\Delta\upsilon_y^2)}/2$. Both of frequency maps verify that the dynamic aperture is large enough for the requirement of injection with |x| ~ 15 mm.

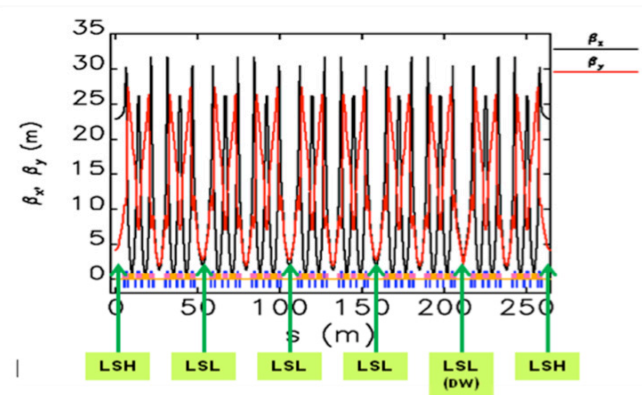

Figure 5: The lattice functions of 1/3 of the ring for working point (37.18, 16.2).

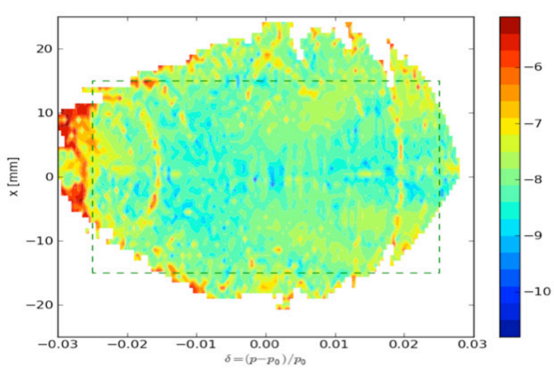

Figure 6: Frequency map in the (x, δ) space.

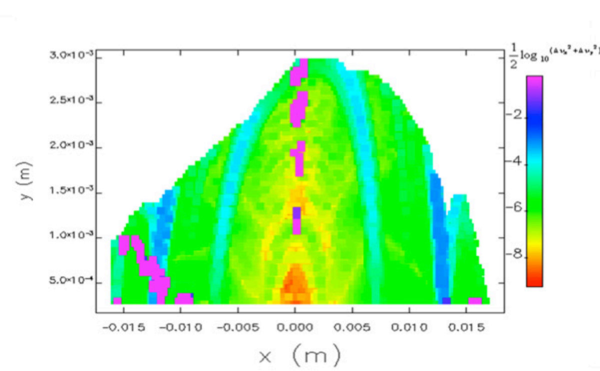

Figure 7: Frequency map in the (x, y) space for on-momentum particle.

The fractional tune footprint (ν_x, ν_y) for the same particles in frequency map Figure 6 is plotted in Figure 8. All particles are stable and have survived after 2048 turns. This shows there are no strong resonances for particles moving with the transverse and longitudinal initial positions.

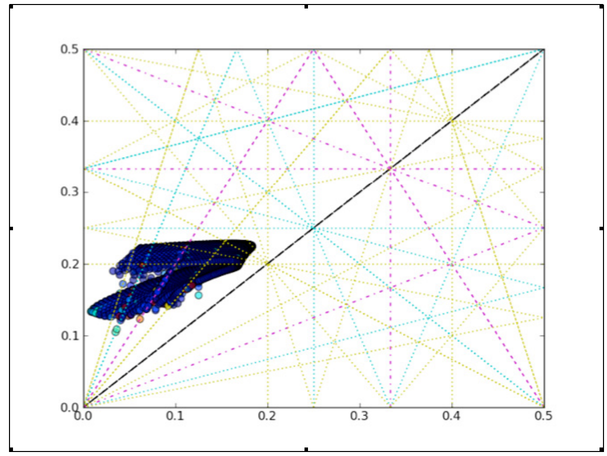

Figure 8: The fractional tunes footprint (ν_x,ν_y).

CONCLUSION

This paper discusses dynamic aperture optimization for the NSLS-II lattice with alternate high and low horizontal beta function in the long straights, which is proposed for the optimization of the brightness of insertion devices. The linear optics is optimized to meet the requirements of lattice function and source properties. Nonlinear optimization for a lattice with working point at (37.18, 16.2) is performed. Considering the realistic magnets errors and physical apertures, we calculate the frequency maps and plot the tune footprint. The results show that the lattice with high-low beta function has adequate dynamic aperture for good injection efficiency and sufficient Touschek lifetime.

REFERENCE

[1] NSLS-II Preliminary Design Reports.

[2] W.Guo, “Tunability of the NSLS-II Lattice”, NSLS-II technical note.

[3] M.Borland, http://www.aps.anl.gov/Accelerator_Systems_Division/Operations_Analysis/oagSoftware.shtml.

[4] J. Bengtsson, “The Sextupole Scheme for the Swiss Light Source (SLS): An Analytic Approach, ” SLS Note 9/97.

[5] J. Bengtsson, “NSLS-II: Control of Dynamic Aperture”, NSLS-II technical report, BNL-81770-2008-IR.

[6] W.Guo, “Re-examination of the misalignment tolerances”, NSLS-II technical report.

[7] L. Yang, “Tracking Code Development for Beam Dynamics Optimization”, PAC11.